

***SH* propagator matrix and Q_S estimates from borehole- and surface-recorded earthquake data**

Jeannot Trampert,* Michel Cara and Michel Frogneux

Institut de Physique du Globe, 67084 Strasbourg Cedex, France

Accepted 1992 August 4. Received 1992 March 26; in original form 1992 January 6

SUMMARY

A new method is proposed for the solving of elastic and anelastic parameters of a medium between two seismometers, one in a borehole and one at the surface. This allows us to retrieve equivalent quality factors of the materials and, at the same time, gives wave velocities as well as reflection and transmission coefficients in a layered structure. The study of local site effects shows that the quality factor of shallow materials can be completely masked by resonance effects and near-surface amplification. Our method is based on the inversion of the *SH* propagator matrix in the time domain. This separates the effects of resonance and amplification in the elastic structure from those of attenuation due either to scattering or physical attenuation, and we find that the elastic problem is decoupled from the anelastic one. After a synthetic test, we applied the method to seismic records made with a borehole-surface instrument operated in the Southern Rhine Graben valley, on the French–German border. Due to high seismic noise at the surface, we were only able to resolve a one-layered mean 500 m deep structure between the borehole and surface instrument. An apparent Q_S of 40 is found between 1 and 5 Hz, a frequency band where classical methods failed. This is in close agreement with Q_S at frequencies larger than 15 Hz obtained from the classical method based on the slope of spectral ratios.

Key words: inversion, propagator matrix, quality factor, site effect.

INTRODUCTION

Borehole seismology probably started in the fifties, when the Naval Ordnance Laboratory (NOL) started investigating microseismicity (Melton 1981). The NOL designed its own seismometers to go down a hole, but technical problems made it difficult to operate them in field conditions. The continuing interest in Earth noise as a function of depth, about 10 years later, led to the development of a borehole seismometer based on the Benioff design. This allowed Douse (1964, 1966) to make a detailed study of the characteristics of seismic noise with depth at frequencies higher than 5 Hz. Long period borehole seismology had to face problems such as larger dimensions of the sensors and different designs of horizontal and vertical components. From all these considerations came a new seismometer design known under the name of ‘Symmetrical Triaxial Seismometer’ (Melton & Kirkpartick 1970). This technology was successfully implemented in a Soviet borehole seismometer and operated over 10 years in a 1000 m deep

well in Kazakhstan (Galperin, Nersesov & Galperina 1986). In 1970 the first practical borehole seismometer was successfully commercialized under the name of ‘Geotech Model 36 000’. These broad-band seismometers were put in service world-wide by the Seismic Research Observatory (SRO) described by Peterson *et al.* (1976).

For local seismic studies, the different research groups tend to design their own downhole packages with inexpensive geophones. Archuleta (1986) compared corner frequencies and analysed spectral ratios between surface and downhole recordings which showed *S*-wave amplifications of 3.5 for the last 35 m of propagation. Hauksson, Teng & Henyey (1987) used a three-level downhole array to study site responses, local quality factors and cut-off frequencies of acceleration spectra. Talebi & Cornet (1987) monitored fluid injection induced microseismicity in a granitic rock mass. Malin *et al.* (1988) analysed velocity spectra and particle motion as a function of depth. Seale & Archuleta (1989), and Blakeslee & Malin (1991) studied several seismic sites and observed frequency responses with a six times average amplification of *S* waves, dominated by reverberation below 10 Hz and attenuation at higher frequencies. Grasso & Wittlinger (1990) used a 3.2 km deep

* Present address: Department of Earth Sciences, 3 Parks Road, Oxford OX1 3PR, UK.

borehole instrument to achieve a better depth location of earthquakes recorded during the monitoring of a gas field in the years 1982–1983. Fletcher *et al.* (1990) studied near-surface velocities and attenuation in boreholes. Blakeslee & Malin (1990) characterized the coda waves from surface versus subsurface seismometers to solve for coda Q . Aster & Shearer (1991a, b) studied polarizations, and modelled site effects for attenuation with three level borehole stations in the San Jacinto fault zone, Southern California.

The main purpose of this paper is to develop an inversion technique of spectral ratios in the time domain using propagator matrices. This allows us to retrieve equivalent quality factors of the materials and at the same time gives the wave velocities as well as the reflection and transmission coefficients in a layered structure. We are interested in the seismic site effects and elastic as well as anelastic properties of the material structure between a 500 m deep borehole seismometer and a surface instrument with the same characteristics. The quality factor is usually measured on the spectral ratio between the surface and borehole records. The spectral ratio technique (e.g. Bath 1974) uses the fact that the slope of the curve, the amplitude of the logarithm of the ratio versus frequency, is inversely proportional to the quality factor. Several authors (Hauksson *et al.* 1987; Malin *et al.* 1988; Fletcher *et al.* 1990) used this method to retrieve a near-surface quality factor from borehole data. Generally, these quality factors are low and vary between 10 and 50 for superficial structures. The study of the local site effect, while important for seismic engineering, shows that the quality factor can be completely masked by resonance effects and near-surface amplification (Seale & Archuleta 1989; Fletcher *et al.* 1990; Blakeslee & Malin 1991). Our new method integrates full wave theory in a layered structure and enables us in particular to separate reverberation from attenuation.

1 LOCAL SITE EFFECT

The Earth's motion in a specific site can be described by a seismic source model propagated by the Green's function of the medium to the recording site. Experimentally, it is seen that Green's function strongly depends on the geological constitution just beneath the recording site. This local property of Green's function is known as the local site effect of the seismic station. The frequency response of the site or transfer function are of first importance for seismic engineering. In places of high seismicity, like California, records of medium to strong earthquakes can be used to establish maps of maximum predicted earthquake shaking. In places of low seismicity, like the Southern Rhine Graben, where the recurrence of strong earthquakes is estimated at several hundred years (Ahorner & Rosenhauer 1978), transfer functions of site effects can be very valuable for making objective estimations of predicted maximum shaking in cases of big earthquakes.

Recent observations with borehole instruments in sedimentary sites indicate that high amplifications of seismic waves occur during the last several hundred metres of propagation (Archuleta 1986; Hauksson *et al.* 1987; Seale & Archuleta 1989; Blakeslee & Malin 1991). In October 1988, we installed a seismic borehole station in the Southern

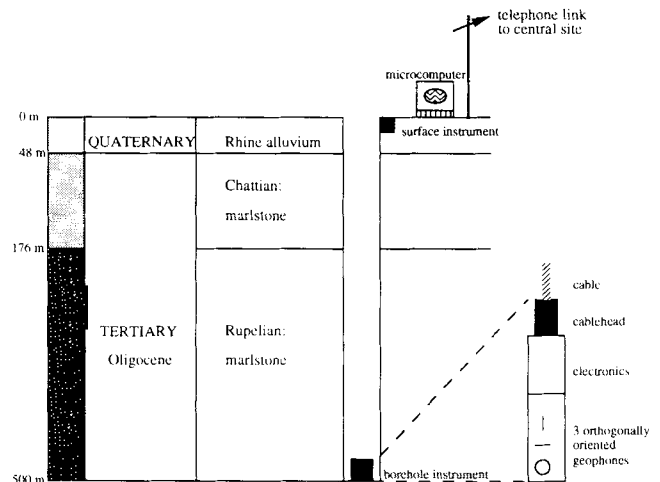


Figure 1. Schematic diagram of the downhole seismic station in the Southern Rhinegraben showing the geological structure of the site and the technical equipment. A brief description of the station can be found in the appendix.

Rhine Graben. The sedimentary structure of the recording site and the station equipment are shown on Fig. 1, and a typical seismic record can be seen on Fig. 2. These seismograms are characterized by two main features:

- (1) a complicated, highly amplified surface signal which needs an explanation other than a simple free surface effect.
- (2) A relatively simple borehole record, summarized by an initial wavelet followed by its surface reflection.

This record can now be used to derive the transfer function of the site. A transfer function gives the total output of a filter for a unit input. The geological structure of our recording site acts as a filter on the upgoing waves to produce the observed surface record. We want the total effect on the surface for a unit perturbation at a 500 m depth. The spectral ratio of the surface signal over the borehole signal does not give the right answer. The borehole signal consists of upgoing and downgoing waves reflected at the free surface and at intermediate layers. Taking the whole borehole signal would introduce information in the transfer function from energy which never reached the surface. In fact, the spectral ratio of the total surface over borehole record gives a measurement of the propagator as we will see below. To get the transfer function of the site effect, we have to deconvolve the surface signal from upgoing waves only.

We assume that the only upgoing wave is the first wavelet of the borehole record (Fig. 2). The spectral ratio of the total surface record over the first wavelet of the borehole record gives the transfer function. Fig. 3 shows the amplitude of the SH transfer function of the site effect for the Southern Rhine Graben. This transfer function has two main features:

- (1) a mean amplification of about 8 for most frequencies. This corresponds to nearly one order of magnitude in earthquake size.
- (2) Superimposed characteristic spikes reaching an amplification of 15. Most of these spikes can be explained with a 48 m alluvium layer and a 176 m Chattian

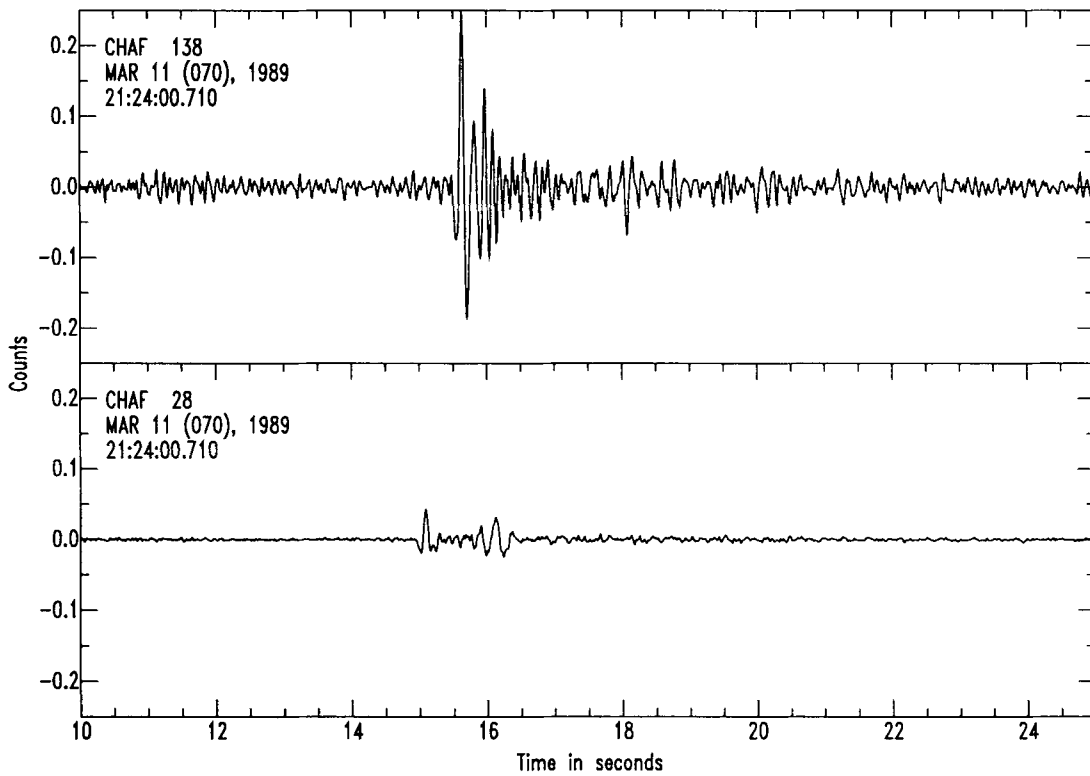


Figure 2. Characteristic *SH* wave recorded at the surface (top) and in the borehole (bottom). The seismograms corresponds to a magnitude 2.7 earthquake which occurred at a distance of 39 km from the station.

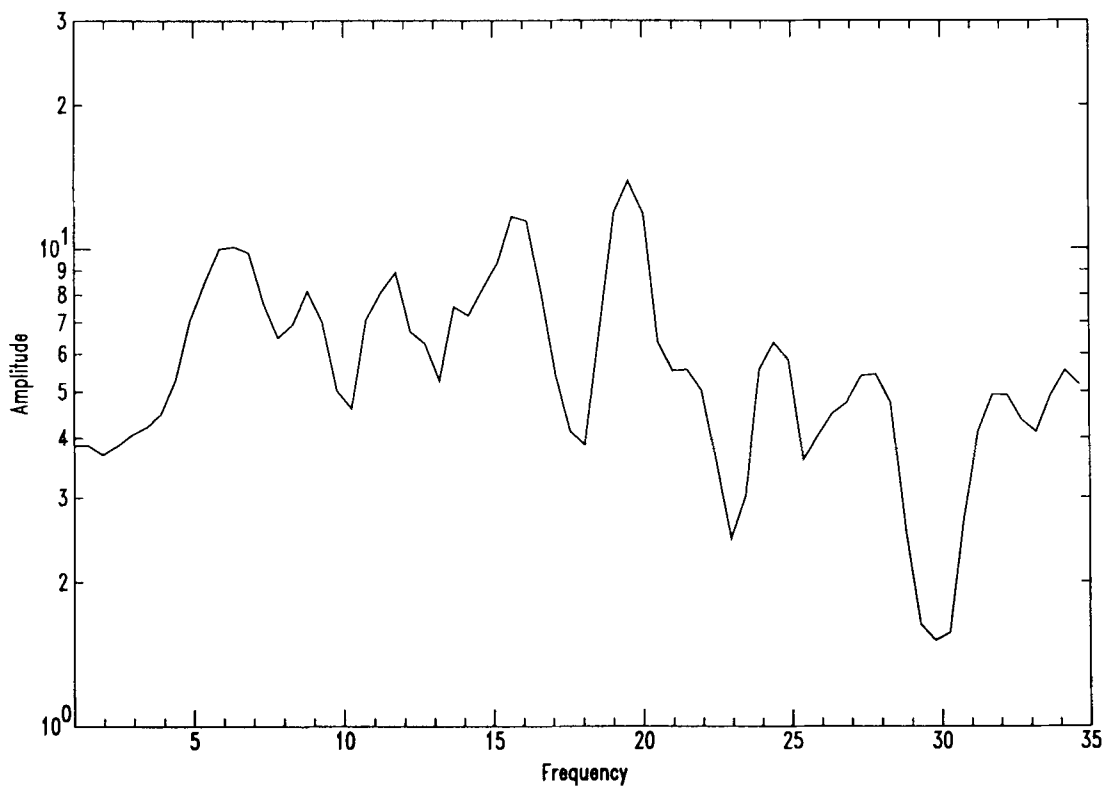


Figure 3. Amplitude of the horizontal transfer function of the site effect deduced from a stack of records.

marlstone layer (Fig. 1) resonating on top of a half space. This is a strong argument in favour of resonance effects.

The average transfer function of our site would seem ideal to estimate the quality factor located between the borehole and surface instruments by measuring its slope and thus first order attenuation (Bath 1974). Unfortunately, up to about 15 Hz, this slope is completely masked by resonance effects. Above 15 Hz, we can clearly identify a slope in the transfer function. Blakeslee & Malin (1991) noticed a similar pattern in their records: low frequency attenuation masked by resonances, whereas high frequencies are dominated by the quality factor of the medium. Seale & Archuleta (1989), and Aster & Shearer (1991b) directly modelled the spectral ratio in the frequency domain to get Q between two instruments at different depths. They observed a good fit at high frequencies but left some low frequency structures unmodelled. This is probably the same phenomena which is responsible for the constant exponential decay of high frequency acceleration spectra observed by Anderson & Hough (1984). They found a striking correlation between this decay and the geological structure of the site. A straightforward application of the spectral ratio technique to all our records gives a consistent quality factor of about 40 for our SH data between 15 and 35 Hz for the medium between the surface and a depth of 500 metres. At lower frequencies, this technique gives inconsistent results.

2 PROPAGATOR INVERSION

Seismic profiles around the station have shown that the sedimentary layers are quasi-horizontal over several tens of kilometers (e.g. Edel *et al.* 1975). For the wavelengths we are going to consider (50–1000 m), it is legitimate to describe our medium by a horizontally layered structure. We assume each layer to be homogeneous to avoid scattering effects which are difficult to separate from intrinsic attenuation. The medium then has only depth dependent properties. The direct problem is formulated with propagator matrices introduced into seismology by Thomson (1950) and Haskell (1953) and generalized by Gilbert & Backus (1966). This method has the advantage of modelling all resonance effects due to layering and near-surface amplifications due to impedance contrasts by considering the exact reflection and transmission coefficients. The waves are supposed to be plane, so that no geometrical spreading occurs.

The attenuation of seismic waves is due to both scattering and physical attenuation, but it is difficult to separate both effects (e.g. Aster & Shearer 1991b). Both types of attenuation can be described by an equivalent anelastic medium, a theory extensively reviewed by Minster (1980), and Ben-Menahem & Singh (1981). Borchardt (1973) studied 3-D wave propagation to find that the Fourier transform of the Navier equation has the same form in an anelastic or an elastic medium, except that in the anelastic case the moduli are complex. To each formal solution in the elastic case corresponds a solution in the anelastic case. This is known as the correspondance principle, although physically wave propagation is completely different in the two cases. Causality requires that the real and imaginary parts of the moduli of the medium have to form a Hilbert

transform pair which only exists if the quality factor is frequency dependent (e.g. Futterman 1962). Seismological observations are in a limited frequency band and Azimi *et al.* (1968) proposed a Hilbert pair where the quality factor Q and the shear wave velocity β are constant over a certain frequency band without violating the causality principle. In that case, the S -wave quality factor Q_s may be written as a frequency independent quantity:

$$Q_s = \frac{\mu_r}{\mu_i} \equiv \frac{\beta_r}{2\beta_i} \quad (1)$$

where the subscripts r and i mean real and imaginary part respectively. μ is the shear modulus and β the shear wave velocity in the considered layer.

The direct problem naturally decomposes in SH and coupled P - SV waves. The following propagator inversion is valid for the SH case only, because the propagator must be built from model parameters uncorrelated to the data. The general solutions in terms of propagator matrices of the equations of motion are given by Gilbert & Backus (1966). In the SH case, the propagator is a (2×2) matrix and the boundary conditions state that the surface is stress free, so that

$$y(z, \omega) = P_{11}(z, 0, \omega) \cdot y(0, \omega) \quad (2)$$

which relates the Fourier transform y of the displacement associated with the SH wave at a depth z to the Fourier transform of the same displacement at the surface via the first diagonal element of the propagator matrix. The spectral ratio of the downhole record over the surface record (which is the inverse spectral ratio normally used in quality factor determinations) completely determines the medium between the two records. In an anelastic halfspace, the propagator for a depth $z = h$ is given at the first order by (Trampert 1990):

$$P_{11}^{(1)}(z, 0, \omega) = 1/2 \left[e^{i\omega \frac{h \cos(j)}{\beta}} \cdot e^{|\omega| \frac{h \cos(j)}{2Q\beta}} + e^{-i\omega \frac{h \cos(j)}{\beta}} \cdot e^{-|\omega| \frac{h \cos(j)}{2Q\beta}} \right]. \quad (3)$$

Equation (3) shows that P_{11} only depends on the model parameters: the layer thickness h , the real part of the shear wave velocity β , the incidence angle j and the quality factor Q given by (1). From equations (2) and (3), we may say that our medium is completely determined by the spectral ratios of our records, and we may write that $g(\mathbf{m}) = \mathbf{d}$, where g is the theoretical relationship (3) between the model parameters \mathbf{m} and the data \mathbf{d} . The inverse problem is then to find g^{-1} , so that $\mathbf{m} = g^{-1}(\mathbf{d})$. Unfortunately, g is highly non-linear in all model parameters, and there is no obvious way to compute g^{-1} .

Noticing that the inverse Fourier transform of a complex exponential is a delta function, motivated us not to look at (3) in the Fourier space, but in the time domain. A similar idea has been proposed by Gir, Gir Subash & Choudhury (1978) who studied the whole crust with teleseismic P waves from spectral ratios between vertical and horizontal components. Instead of taking the inverse Fourier transform, they took the Fourier transform of the amplitude of the spectral ratio called 'cepstrum'. By neglecting the phase, however, they lost the information concerning the quality factor. The only mathematical complication in the inverse Fourier transform of (3) comes

from the real exponentials. The corresponding integral is divergent when its argument is positive. The result is that the general solution (2) of the equation of motion is constructed as a superposition of up- and downgoing waves. Suppose that an upgoing wave travels from the depth z to the surface. In an absorbing medium, its corresponding amplitude will decrease. The way the wave problem is solved, we explain the borehole record (depth z) by applying the surface record to the propagator. To do this, we have to take an upgoing wave at the surface and amplify it during the back-propagation to obtain the right initial amplitude at the borehole location. Obviously, waves at infinite frequencies need infinite amplification, which means that the integral will diverge. To avoid this problem, we propose to introduce a cut-off frequency, so that we have a smoothed vision of our medium. In other words, the cut-off frequency will fix a minimum layer thickness which can be detected by the waves. We may then write the temporal propagator corresponding to (3) as

$$P_{11}^{(1)}(z, 0, t) = 1/2 \left\{ \delta \left[t - \frac{h \cos(j)}{\beta} \right] * FT^{-1} \left[c(\omega_0) \cdot e^{-|\omega| \frac{h \cos(j)}{2Q\beta}} \right] \right. \\ \left. \times \delta \left[t + \frac{h \cos(j)}{\beta} \right] * FT^{-1} \left[c(\omega_0) \cdot e^{|\omega| \frac{h \cos(j)}{2Q\beta}} \right] \right\} \quad (4)$$

where c is a boxcar function which is 1 between the cut-off frequencies $-\omega_0$ and $+\omega_0$, and 0 elsewhere. Equation (4) represents two spikes dispersed in time. The positions of the two spikes are symmetric in time with maximum amplitude at the central points $-h \cos(j)/\beta$ and $+h \cos(j)/\beta$ respectively. To carry out the remaining integration in (4), we explicitly need to introduce the frequency dependence of Q and β . We have chosen Q and β constants over a the bandwidth of interest. The inverse Fourier transforms of the attenuation terms at their central points are of the form

$$\frac{1}{2\pi} \int_{-\omega_0}^{\omega_0} e^{|\omega|x} \cdot e^{i\omega t} \cdot d\omega = \frac{e^{\omega_0 x} - 1}{\pi x} \\ \frac{1}{2\pi} \int_{-\omega_0}^{\omega_0} e^{-|\omega|x} \cdot e^{i\omega t} \cdot d\omega = \frac{1 - e^{-\omega_0 x}}{\pi x} \quad (5)$$

and it is then easy to show that the amplitude ratio r_1 of the two spikes at their central points is given by:

$$\text{Log}(r_1) = \omega_0 \frac{h \cos(j)}{2Q\beta} \quad (6)$$

The interesting result is that the elastic part of the problem is completely determined by the position of the spikes on the time axis, and the anelastic part is given by the amplitude ratio at the central points.

To generalize the above formulae, let us analyse how the temporal propagator is constructed. The wave equation is solved in a way that the total seismogram at depth z is the result of the temporal propagator convoluted to the total surface signal. The temporal propagator is then the solution of the wave equation at depth z for a Dirac delta function propagated downwards. Furthermore, the initial wave equation is a second order differential equation in time so that the elastic part of the solution has to be symmetric in time. Fig. 4 outlines the general procedure to construct P_{11} . Starting from a delta function at the surface at time 0, the temporal propagator at the base of the first layer consists of two spikes (equation 4) at positions $-\eta_1$ and $+\eta_1$, where $\eta_1 = h_1 \cos(j_1)/\beta_1$ is the vertical traveltime in the first layer. In a purely elastic medium, the spikes would be delta functions with half the surface amplitude. The anelasticity introduces the asymmetry of amplitudes in time and disperses the delta functions. The spike propagated in the negative time direction is amplified while the positively propagated one is attenuated. The spike at $-\eta_1$ gives two spikes positioned at $(-\eta_1 - \eta_2)$ and $(-\eta_1 + \eta_2)$. It is easy to show that the elastic amplitudes now depend on the reflection and transmission coefficients as shown on Fig. 4. The same happens to the spike at $+\eta_1$ to respect the symmetry of the elastic part of the solution. All amplitudes are modified by the propagation with different times in an attenuating medium. Because the elastic part of the solution is symmetric in time, the amplitude ratio of two spikes symmetric in time only depends on the quality factors of the medium. The amplitude ratio of two spikes, non-symmetric in time, gives the reflection and transmission coefficients, but needs correction for different attenuation.

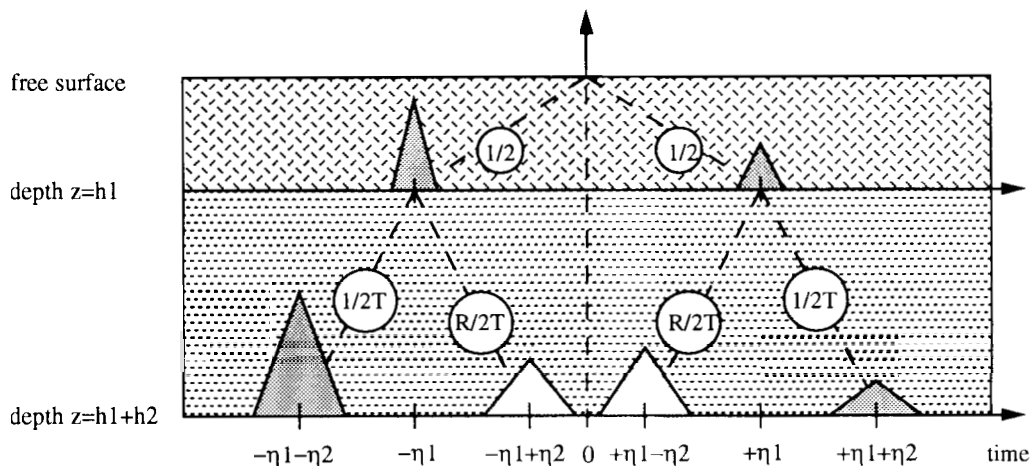


Figure 4. Construction of the temporal propagator. The expressions in circles describe the evolution of the elastic amplitudes of the downwards propagated unit delta function, where R and T are the reflection the transmission coefficients between the two layers. The amplitudes are further modified by the effects of anelasticity.

Following the procedure outlined on Fig. 4, we derived a general expression for the temporal propagator corresponding to an n -layered structure based on the results of an $(n-1)$ -layered medium:

$$p_{11}^{(n)}(z, 0, t) = \sum_{i=1}^{2^{n-1}} a_i^{(n)} \cdot \{ \delta[t - H_i^{(n)}] * FT^{-1}[c(\omega_0) \cdot e^{-i\omega A_i^{(n)}}] + \delta[t + H_i^{(n)}] * FT^{-1}[c(\omega_0) \cdot e^{i\omega A_i^{(n)}}] \} \quad (7)$$

with

$$\left\{ \begin{array}{l} \eta_n = \frac{h_n \cos(j_n)}{\beta_n} \\ \alpha_n = \frac{h_n \cos(j_n)}{2Q_n \beta_n} \\ H_{2i-1}^{(n)} = H_i^{(n-1)} + \eta_n \quad \text{and} \quad H_{2i}^{(n)} = H_i^{(n-1)} - \eta_n \\ A_{2i-1}^{(n)} = A_i^{(n-1)} + \alpha_n \quad \text{and} \quad A_{2i}^{(n)} = A_i^{(n-1)} - \alpha_n \\ A_1^{(0)} = H_1^{(0)} = 0 \\ z = \sum_{i=1}^n h_i \end{array} \right.$$

Expression (7) can be seen as a recursive formula where the vertical propagation times $H_i^{(n)}$ are built from the different η and the reduced vertical traveltimes $A_i^{(n)}$ from the different α corresponding to an $(n-1)$ -layered medium. The $a_i^{(n)}$ are functions of the reflection and transmission coefficients between the different layers. The temporal propagator (7) represents 2^n spikes dispersed in time, organized in pairs symmetric in time. The measurement of the central points allows us to solve η_i , and the corresponding amplitude ratio is a function of the Q_i in the different layers, and it is easily shown that

$$\text{Log}(r_i) = \omega_0 A_i^{(n)} \quad (8)$$

where r_i is the amplitude ratio at the central position for one of the 2^{n-1} pairs of spikes. Knowing the different η_i independently, allows us to invert (8) to get the different Q_i of our n layers. In principle it is possible to relate the amplitude ratios of spikes, non-symmetric in time, to the reflection and transmission coefficients between the different layers, but this involves long algebra, and the development is not shown here.

From a highly non-linear and coupled elastic-anelastic problem, we obtained a completely linear decoupled problem in (7) and (8). This shows the important fact, that a problem is not linear or non-linear in itself, but only its formulation.

We now have all the necessary tools to invert the propagator for the elastic and anelastic parameters of the medium, and before applying the method of our data, we briefly summarize the technique:

(1) first, we compute the spectral ratio of the borehole record over the surface record. Then we choose a cut-off frequency, which will determine the equivalent medium that we can solve with the considered frequencies. Next, we compute the inverse Fourier transform up to the frequency ω_0 .

(2) We observe a certain number of spikes, organized in pairs symmetric in time. The total number of spikes (2^n) immediately gives the number of layers n which have been seen by the waves. With our seismograms recorded in the

Southern Rhine Graben, we had to restrict the method to a single layer because of a low signal-to-noise ratio in the observed spectral ratios.

(3) The positions of the 2^{n-1} pairs on the time axis correspond to the different values H_i and give the n elastic parameters η_i . The association of a given spike with a given H_i can be difficult if we are dealing with a great number of layers, but is no problem for a relatively simple medium, made out of a few nearly homogeneous layers.

(4) Once the η_i are known, we can solve h_i or β_i , if we know β_i or h_i respectively from an independent source (e.g. geological log, velocity analysis, . . .). The incidence angles j_i can normally be measured either at the surface or at the downhole instrument.

(5) The 2^{n-1} amplitude ratios for the different pairs give through (8) the different quality factors for all the layers. Remember that the frequency dependence of Q and β has to be explicitly stated (constant over a certain bandwidth here) to derive (8). We may then write that $\mathbf{d} = \mathbf{Gm}$, where \mathbf{d} is the amplitude ratios, \mathbf{G} is the matrix of the partial derivatives made from the different η_i and \mathbf{m} is the vector built with the inverse quality factors. This classical linear inverse problem can be solved by any algorithm (e.g. Tarantola 1987).

(6) Eventually, reflection and transmission coefficients can be found by a linear combination of amplitude ratios from different pairs. It can be shown that these coefficients only depend on objective measurements of amplitude ratios and are independent of spike positions (η_i) and quality factor determinations.

The approach followed by Gir *et al.* (1978) can be compared up to point (4) of our method, but loses all information on amplitudes to get a quality factor or reflection and transmission coefficients.

3 RESULTS

We computed a theoretical temporal propagator in a two-layered medium where a 50 m thick layer with an S -wave velocity of 400 m s^{-1} , a density of 2200 kg m^{-3} and a quality factor of 40 lies on top of a 450 m thick layer with an S -wave velocity of 1000 m s^{-1} , a density of 3200 kg m^{-3} and a quality factor of 100. This gives a reflection coefficient of 0.551 between the two layers. The plane wave arrives from below with an incident angle of 20° , and we have chosen a cut-off frequency of 15 Hz. Fig. 5 shows the results for a non-causal propagator, where Q and β are constant in the two layers and a causal one obtained with the dispersive relations given by Azimi *et al.* (1968). The two are very similar which justifies an interpretation of our real temporal propagators (which are causal) with equations (7) and (8) obtained from a constant Q and β . The reader easily checks that we retrieve the introduced structure within 5 per cent.

From about 25 local earthquakes ($<100 \text{ km}$ distance) recorded so far, five records had a high enough signal-to-noise ratio at the surface to identify most seismic phases. Our station is located in a highly industrialized area with an exceptionally high surface noise. The SH wave could be clearly identified on two surface seismograms only. Primarily, we are interested in the mean structure between the surface and downhole instrument, in order to compare

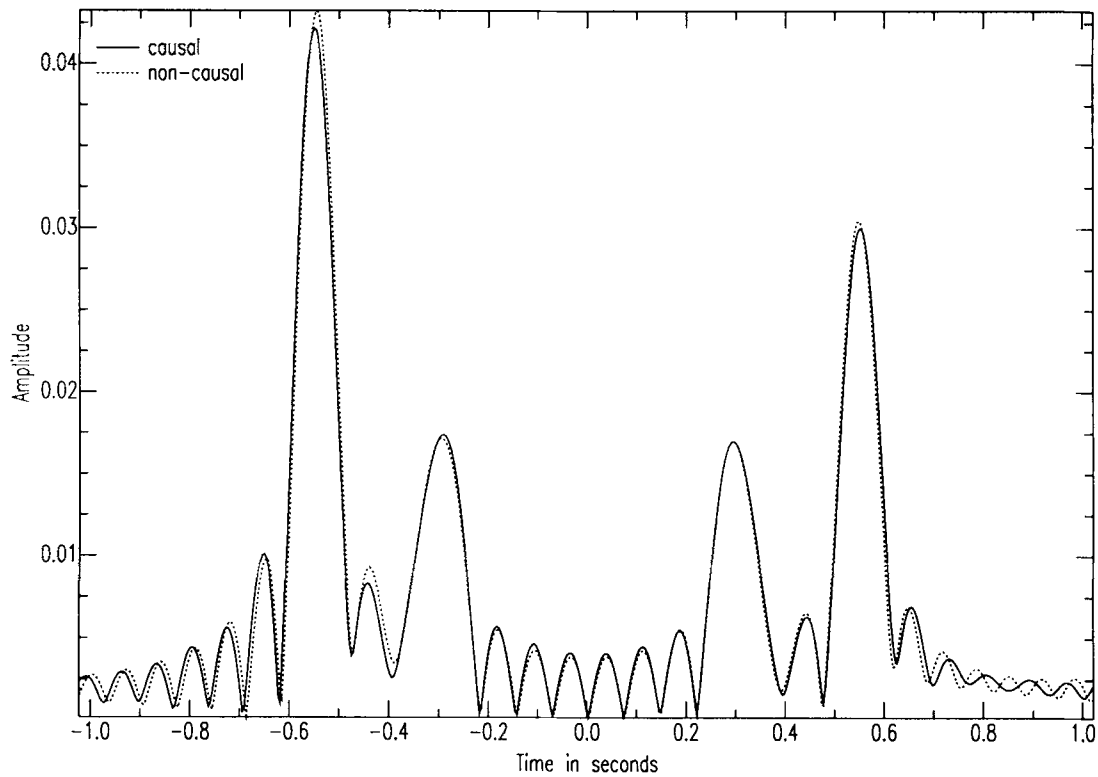


Figure 5. A causal and non-causal theoretical temporal propagator for a 2-layered medium described in the main text. The low amplitude spikes are due to the Gibbs effect introduced by the cutoff frequency.

the results with independently obtained parameters. Consequently we have chosen a cut-off frequency of 5 Hz. Figs 6(a) and 6(b) show the *SH* records together with the corresponding temporal propagators. We observe two spikes for each propagator, which indicates that the waves up to 5 Hz have indeed seen a mean structure of one layer. It is difficult to observe additional spikes due to the poor signal-to-noise ratio of the surface records. In particular, we are not able to retrieve the second pair of spikes expected from the theoretical modelling of the alluvium layer (Fig. 1). The position of the spikes on the time axis (equation 4) measures $h \cos(j)/\beta$, and knowing h (500 m), we get $\beta/\cos(j)$. We measured the incidence angle at the downhole instrument on a 3-D particle motion plot and found an incidence angle of about 25° for both events. This yields an *SH*-wave velocity of 860 m s^{-1} for our medium. A sonic log taken during the drill of the borehole gave a mean *P*-wave velocity of 2700 m s^{-1} for the same structure, and we then get a V_p/V_s ratio of 3.14. This is in good agreement with the V_p/V_s ratio of 3.26, obtained independently from the *P*- and *S*-wave arrival times read on our records. Using the measured values of $h \cos(j)/\beta$ and the amplitude ratios of the spikes on Fig. 6, we solved equation (4) for Q_s and obtained 40. This quality factor is valid between 1 Hz (cut-off frequency of our seismometers) and 5 Hz (cut-off frequency for the temporal propagator). This low frequency quality factor is equal to the quality factor obtained from the transfer function of the site effect between 15 and 35 Hz. It is worth noticing that the classical spectral ratio method failed completely at frequencies smaller than 15 Hz, even a more sophisticated direct modelling of spectral ratios failed

at lower frequencies as reported by Aster & Shearer (1991b).

CONCLUSION

We propose a new method, based on the inversion of the *SH* propagator matrix in the time domain, to solve for elastic and anelastic parameters of a medium between two vertically separated seismometers, one being at the surface. The method applies to a horizontally stratified medium and gives as part of the solution the number of layers objectively. The temporal propagator consists of a certain number of spikes organized in pairs symmetric in time. The position of the spikes on the time axis depends only on the velocity and thickness of the different layers. The amplitude ratio between two spikes symmetric in time are related to quality factors of the different layers. It is possible to obtain the reflection and transmission coefficients in the medium from the amplitude ratios of spikes non-symmetric in time. All model parameters can be solved with classical linear inversion techniques.

In this paper, the method is applied to the first local earthquakes recorded at the surface and at the bottom of our borehole station in the Southern Rhine Graben. The results corresponding to a one-layered structure are in agreement with results from more classical approaches and extend where classical methods fail. An apparent Q_s of 40 is found in this 500 m thick water-saturated sedimentary medium for the frequency range between 1 and 5 Hz, which is in agreement with Q_s obtained at frequencies larger than 15 Hz from the slope of the spectral ratios. We find an

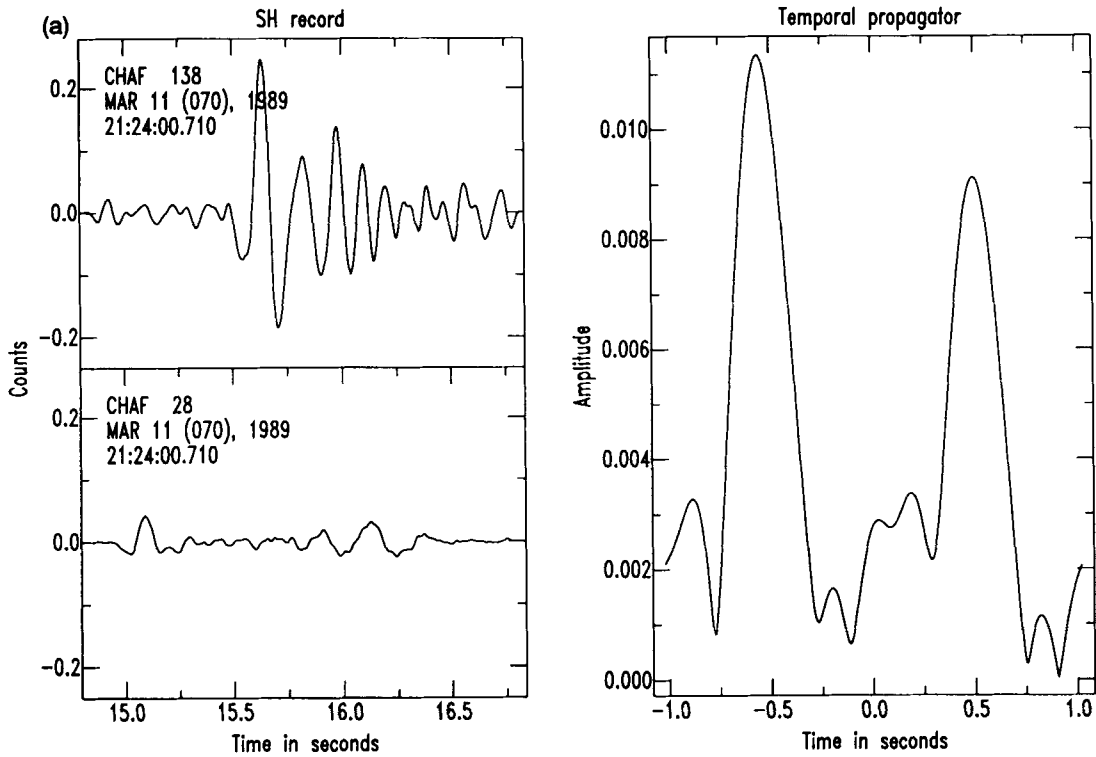


Figure 6(a). SH record with corresponding temporal propagator at a cut-off frequency of 5 Hz. The propagator carries information of the elastic and anelastic structure lying between the borehole and the surface instrument. The corresponding earthquake has a magnitude of 2.7 and is at a distance of 39 km from the station.

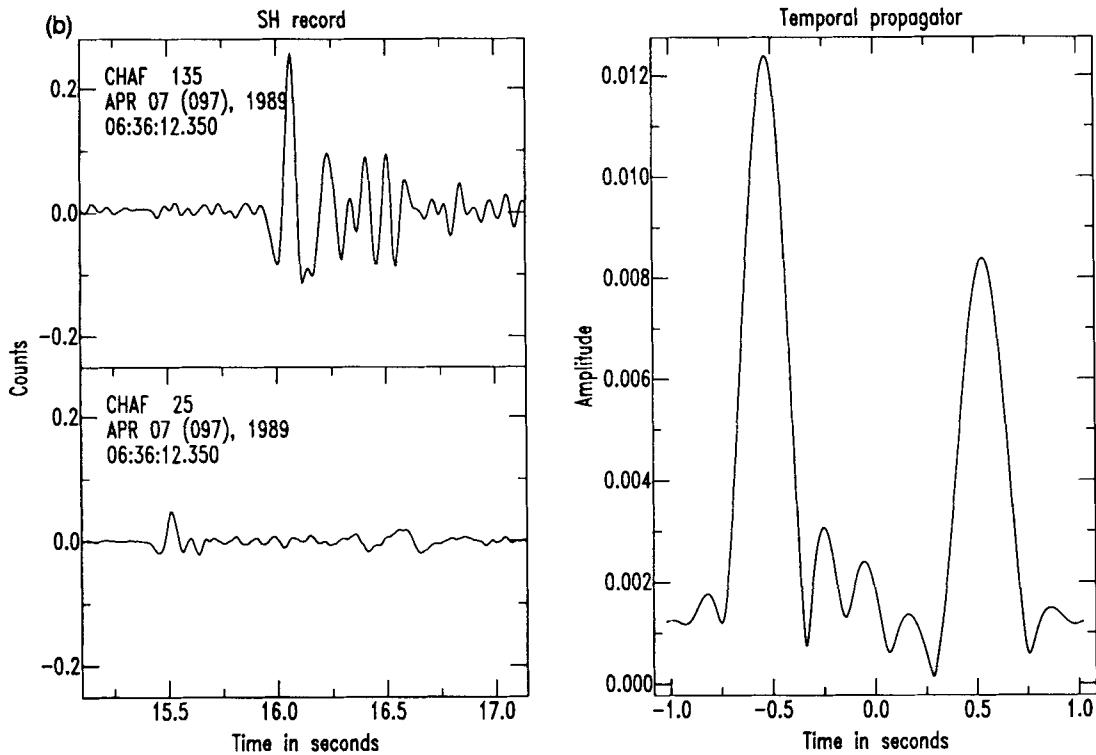


Figure 6(b). Same as Fig. 6(a) for an earthquake of magnitude 2.5 and a distance of 43 km.

SH-wave velocity of 860 m s^{-1} which yields a V_p/V_s ratio of 3.14, or equivalently a Poisson ratio of 0.44. This is confirmed by an independent study of *P*- and *S*-wave arrival times, and indicates that the medium is not very rigid. The site effect shows a clear overall amplification of a factor of 8 for *SH* waves, superimposed on which are characteristic spikes due to resonance effects with much larger amplification. Most of these spikes are in the frequency range of buildings and should not be underestimated.

ACKNOWLEDGMENTS

We wish to thank Mr Aubert and Mr Bouquerelle from INSU for their continuous support to this project, and F. Cornet and L. Martel who helped us in designing the borehole instrument. Mr Schreiber and Mr Lucazeau from MDPA engineered the rescue of the borehole and made geological and well-logging results available to us. Mr Filliot from Chambre de Commerce de Mulhouse and Mr Baumann from Rhone Poulenc helped with many administrative and technical questions. Most of the mechanical work was realized by Gerard Ball. The constructive comments of Peter Malin's review helped to improve this manuscript. This work was conducted under the INSU contract number 88145012.07

REFERENCES

- Ahorner, L. & Rosenhauer, W., 1978. Seismic risk evaluation for the Upper Rhine Graben and its vicinity, *J. Geophys.*, **44**, 481–497.
- Allen, R. V., 1978. Automatic earthquake recognition and timing from single traces, *Bull. seism. Soc. Am.*, **68**, 1521–1532.
- Anderson, J. G. & Hough, S. E., 1984. A model for the shape of the Fourier amplitude spectrum of acceleration at high frequencies, *Bull. seism. Soc. Am.*, **74**, 1969–1993.
- Archuleta, R. J., 1986. Downhole recordings of seismic radiation, in Earthquake source mechanics, *Geophysical Monograph Series*, eds Das Sh., Boatwright J. & Scholtz Ch. H., American Geophysical Union.
- Aster, R. C. & Shearer, P. M., 1991b. High-frequency borehole seismograms recorded in the San Jacinto fault zone, Southern California. Part 2. Attenuation and site effects, *Bull. seism. Soc. Am.*, **81**, 1081–1100.
- Azimi, Sh. A., Kalinin, A. V., Kalinin, V. V. & Pivovarov, B. L., 1968. Impulse and transient characteristics of media with linear and quadratic absorption laws, *Izvestiya, Physics of the Solid Earth*, February, 88–93.
- Azimi, Sh. A., Kalinin, A. V., Kalinin, V. V. & Pivovarov, B. L., 1968. Impulse and transient characteristics of media with linear and quadratic absorption laws, *Izvestiya, Physics of the Solid Earth*, **000**, 88–93.
- Bath, M., 1974. *Spectral analysis in geophysics*, Elsevier, Amsterdam.
- Ben-Menahem, A. & Singh, S. J., 1981. *Seismic waves and sources*, Springer Verlag, New York.
- Blakeslee, S. N. & Malin, P. E., 1990. A comparison of earthquake coda waves at surface versus subsurface seismometers, *J. geophys. Res.*, **95**, 309–326.
- Blakeslee, S. N. & Malin, P. E., 1991. High-frequency site effects at two Parkfield downhole and surface stations, *Bull. seism. Soc. Am.*, **81**, 332–345.
- Borcherdt, R. D., 1973. Energy and plane waves in linear viscoelastic media, *J. geophys. Res.*, **78**, 2442–2453.
- Douse, E. I., 1964. Signal and noise in deep wells, *Geophysics*, **29**, 721–732.
- Douse, E. I., 1966. Noise attenuation in shallow holes, *Bull. seism. Soc. Am.*, **56**, 619–632.
- Edel, J. B., Fuchs, K., Gelbke, C. & Prodehl, C., 1975. Deep structure of the southern Rhine Graben area from seismic refraction investigations, *J. Geophysics*, **41**, 333–356.
- Fletcher, J. B., Fumal, T., Liu, H. P. & Carroll, L. C., 1990. Near-surface velocities and attenuation at two boreholes near Anza, California, from logging data, *Bull. seism. Soc. Am.*, **80**, 807–831.
- Futtermann, W. I., 1962. Dispersive body waves, *J. geophys. Res.*, **67**, 5279–5291.
- Galperin, E. T., Nersesov, I. L. & Galperina, R. M., 1986. *Borehole seismology and the study of the seismic regime of large industrial centres*, D. Reidel Publishing Company, Dordrecht, Holland.
- Gilbert, F. & Backus, G. E., 1966. Propagation matrices in elastic wave and vibration problems, *Geophysics*, **31**, 326–332.
- Gir, R., Gir Subash, S. M. & Choudhoury, M. A., 1978. Investigation of crustal structure by the analysis of reverberation periodicities, *Bull. seism. Soc. Am.*, **68**, 1387–1397.
- Grasso, J. R. & Whittlinger, G., 1990. Ten years of seismic monitoring over a gas field, *Bull. seism. Soc. Am.*, **80**, 450–473.
- Haskell, N., 1953. The dispersion of surface waves on multilayered media, *Bull. seism. Soc. Am.*, **43**, 17–34.
- Hauksson, E., Teng, T. L. & Henyey, T. L., 1987. Results from a 1500m deep three level downhole seismometer array: site response, low *Q* values and f_{max} , *Bull. seism. Soc. Am.*, **77**, 1883–1904.
- Malin, P. E., Waller, J. A., Borcherdt, R. D., Cranswick, E., Jensen, E. G. & Van Schaack, J., 1988. Vertical seismic profiling of Oroville microearthquakes: velocity spectra and particle motion as a function of depth, *Bull. seism. Soc. Am.*, **78**, 401–420.
- Mayer Rosa, D. & Wechsler, E., 1991. The Basel 1356 earthquake: effect on contemporary buildings in the two of Basel, in *Proceedings of the Third International Symposium on Historical Earthquakes in Europe*, ed. Kozak, J., Geophys. Inst. Czech. Acad. Sci., Prague.
- Melton, B. S., 1981. *Earthquake seismograph development: a modern history—Part 1*, EOS, **62**, (21), 505–510.
- Melton, B. S. & Kirkpatrick, B. M., 1970. The symmetrical triaxial seismometer—its design for application to long-period seismometry, *Bull. seism. Soc. Am.*, **60**, 717–739.
- Minster, J. B., 1980. Anelasticity and attenuation, International School of Physics 'Enrico Fermi', Course LXXVIII, in *Physics of the Earth's interior*, pp. 151–212, ed. Dziewonski, A. M. & Boschi, E., North-Holland Publishing Company, Amsterdam.
- Peterson, J., Butler, H. M., Holcomb, L. G. & Hutt, C. R., 1976. The Seismic Research Observatory, *Bull. seism. Soc. Am.*, **66**, 2049–2068.
- Seale, S. H. & Archuleta, R. J., 1989. Site amplification and attenuation of strong ground motion, *Bull. seism. Soc. Am.*, **79**, 1673–1696.
- Talebi, Sh. & Cornet, F. H., 1987. Analysis of the microseismicity induced by a fluid injection in a granitic rock mass, *Geophys. Res. Letters*, **14**, 227–230.
- Tarantola, A., 1987. *Inverse problem theory*, Elsevier, Amsterdam.
- Thomson, W. T., 1950. Transmission of elastic waves through a stratified solid medium, *J. Appl. Phys.*, **21**, 89–93.
- Trampert, J., 1990. Borehole seismology and tomography, *PhD thesis*, University of Strasbourg.

APPENDIX

The Southern part of the Rhine Graben was affected in 1356 by a large destructive earthquake with an estimated magnitude of 6.5 and an epicentre near Basel, Switzerland

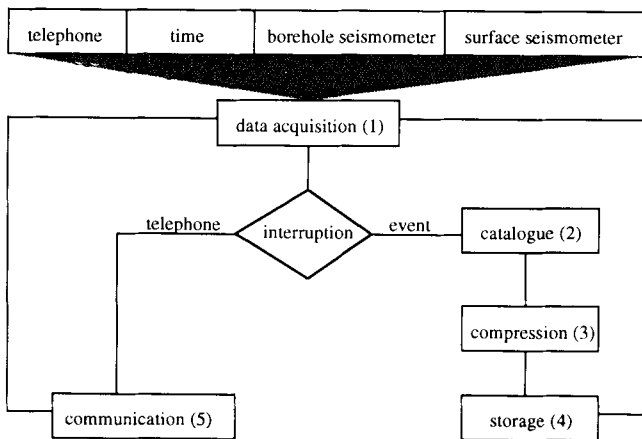


Figure A1. Flow chart of the data acquisition programs in the borehole station.

(e.g. Mayer Rosa & Wechsler 1991). This region is now showing a rather high seismicity compared to its surrounding area (Ahorner & Rosenhauer 1978). Instrumental seismicity is presently surveyed by three short period networks installed by 'Institut de Physique du Globe', Strasbourg; 'Geophysikalisches Institut', Karlsruhe; and 'ETH', Zurich. Because of a high seismic noise in the Rhine valley, most of these stations are installed on the crystalline basement in the near Vosges mountains and Black Forest. The Alsatian Potassium Mines made a 500 m deep borehole available to us. The well is completely cased and the bottom is made out of a 200 m thick concrete plug. It is located in the centre of the Rhine Graben where we installed a downhole station in October 1988. The main geological characteristics of the site were determined during the drilling and are shown on Fig. 1.

We use a three component seismometer developed by 'Lennartz Electronic', the LE-3D. This seismometer is based on 4.5 Hz geophones which are transformed with a feedback system and a bandpass filter to simulate 1 Hz electrodynamic geophones with a damping factor of 0.7, more adapted to seismological means. The LE-3D has several characteristics which make it particularly suitable for a borehole use. The sensors are relatively small 4.5 Hz geophones, which can easily be integrated in a borehole package. Furthermore, small geophones are less sensitive to a tilted installation which cannot be avoided with an unclamped instrument. Finally, the feedback system guarantees a high dynamic range (≈ 130 db). The sensors, protected by a stainless steel housing, are coupled to the borehole floor by gravity. The dimensions of the instrument guarantee a maximum tilt of about 3° for our 7 inch borehole. The complete seismological station (Fig. 1) consists of a 3 component 1 Hz seismometer at a depth of 500 m and an identical instrument at the surface. The time is read on a DCF receiver. A microcomputer is in charge of the data acquisition and the local storage of the detected events on the hard disc. To transfer the data to a central site, we use an ordinary telephone line.

The seismic signals are read by a microcomputer via a 12 bits A/D card. Three gain levels provide an apparent dynamic of 108 db to the data acquisition system. Each channel is sampled with 250 points per second. Furthermore, the PC is connected to a modem used for

communication with the central site. The flow chart of the software is shown on Fig. A1. The data acquisition program (1) is scanning three seismic borehole channels, three seismic surface channels, a time channel and the telephone line. This program can be interrupted by two sources only:

(1) The STA/LTA algorithm (Allen 1978) has detected an event. A catalogue containing all available files on the local disc is updated (2), the event is compressed (3) for future transmission and stored on the hard disc of the station computer (4).

(2) A telephone call is detected, which loads a communication program (5) for data exchange between two computers. The local computer in the seismic station is completely passive during the communication process, and sends or receives files as requested by the central site. This allows an easy data transfer to the central site and a comfortable servicing of the software in the seismic station.

During these two interruptions of the data acquisition program, the seismic channels are not scanned, and there is a chance of missing some events. In two years of nearly continuous operation, we missed two local earthquakes out of 200 while we were communicating with the borehole station. As a security measurement, in the case of a big earthquake or a local seismic crisis, we have a continuous analogical transmission of the vertical downhole component to the central site.

We developed a relative calibration method with a perfectly well known reference seismometer from a shaking table (Trampert 1990). This technique has the advantage that the seismometer excitation function must not be known. This calibration method may be applied to all seismometer types and allows us to check the temporal evolution of a transfer function while the instrument stays operational in the field.

Another instrumental unknown is the orientation of the horizontal components of the borehole seismometer which was lost during the descent of the instrument. We used local earthquakes which were perfectly localized by regional seismic networks. We determined the apparent azimuth of the horizontal borehole components from the particle motion of the first P arrivals, and the difference with the true azimuth gives the horizontal orientation of the downhole instrument. Care has to be taken with polarization studies, as local heterogeneities may deflect ray paths. This is easily checked by repeating the azimuth determinations with the same signals filtered at different bandwidths. The measurements were relatively coherent and gave a standard deviation of 5° for the orientation.

The station has been working without any significant interruption since November 1988. Its complete technical description as well as its performance is described in Trampert (1990). The station is located in a highly industrialized area, and consequently, the seismic noise is extremely strong on the surface. We measured a 20 db mean noise reduction at a depth of 500 metres in the sedimentary structure of the Southern Rhine Graben. This confirms results of other works in sedimentary structures (Galperin *et al.* 1986; Hauksson *et al.* 1987; Malin *et al.* 1988; Aster & Shearer 1991b). Even with this 20 db gain, it has to be said that the noise conditions are still worse than for a seismic station located on crystalline bedrock.